JOURNAL OF SOLID STATE CHEMISTRY 76, 26–32 (1988)

Preparation and Crystal Structure of the Semiconducting Compound $Sn_{4.2}Si_9P_{16}$

JEAN-YVES PIVAN, ROLAND GUERIN, JEAN PADIOU, AND MARCEL SERGENT

Université de Rennes-Beaulieu, Unité Associée au CNRS No. 254, Laboratoire de Chimie Minérale B, Avenue du Général Leclerc, 35042 Rennes Cédex, France

Received November 9, 1987

The phosphide $Sn_{4.2}Si_9P_{16}$ has been grown as single crystals using tin as a flux. The unit cell is rhombohedral, space group $R3$, with $a = 9.504(2)$ Å, $\alpha = 111.00(2)°$, and $Z = 1$. The X-ray structure was solved from three-dimensional single-crystal counter data and refined down the final R indices 0.027 and 0.033 for 854 independent reflections. It consists of $|SiP_4|$ tetrahedra linked together by common apices which generate a tridimensional framework into which tin atoms, in a distorted tetrahedral phosphorus coordination, are inserted. This new compound was found to be semiconducting with a band gap of 0.2 eV. © 1988 Academic Press, Inc.

Introduction

Electrical conductivities of several binary phases containing elements of the fourth and fifth groups have previously been reported (*1*). Among those which are given to be semiconductors are several compounds of AB and AB_2 stoichiometry. Thus, as an example, the Si–P system exhibits both compounds SiP and SiP_2 which crystallize in numerous allotropic forms (*2–6*). In order to prepare new phosphorus-rich silicon phosphides, tin has been used as a flux. The reaction yielded well-developed and large crystals, which belong to a new phase, the formula of which was found to be $Sn_{4.2}Si_9P_{16}$ by structure determination. This compound is semiconducting with a band gap of 0.2 eV. The synthesis, crystal structure, and electrical properties of this new compound will be discussed in detail.

Experimental

Starting materials were elementary silicon, red phosphorus, and tin, all with minimum purity >99.9%. The initial mixtures were sealed under vacuum in quartz tubes, annealed in a vertical furnace at 1050°C for 3 days. They were afterward slow-cooled at rates of 5–10°C/hr down to 600°C and then more quickly (50°C/hr) down to room temperature. Well-developed single crystals were isolated by removing the tin matrix with moderately diluted hydrochloric acid. After rinsing, first in water and then in acetone, the crystals were dried in air at room temperature. Crystals of two different morphology types, viz. initial atomic ratios, were obtained: very thin needles when Sn : Si : P = 1 : 5 : 10 and small truncated octahedra when Sn : Si : P = 1 : 2 : 10.

In the latter case, the single crystals were

0022-4596/88 $3.00

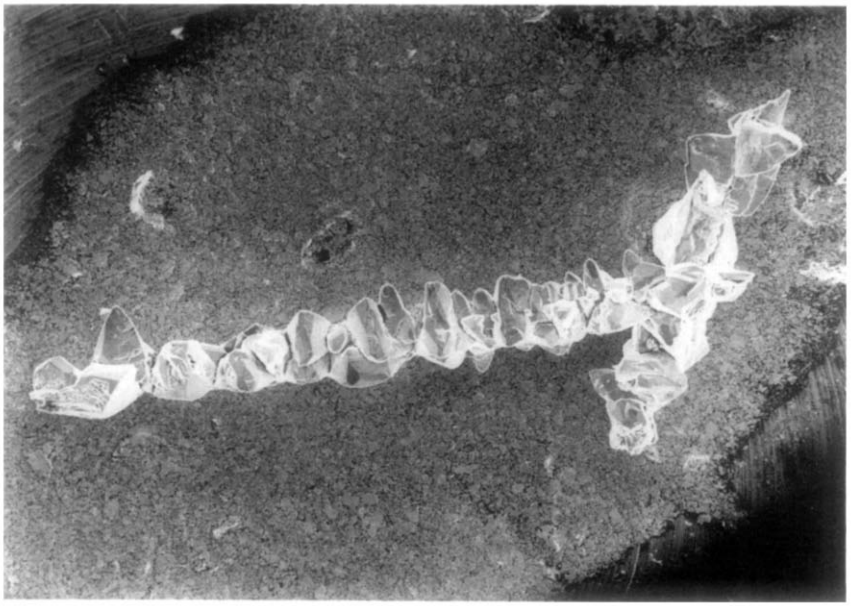

FIG. 1. $Sn_{4.2}Si_9P_{16}$ single crystals as truncated octahedra on their support SiP.

deposited on large and gold-reddish needles of binary SiP (Fig. 1). These crystals were separated from their support by mechanical means. When increasing the phosphorus content, no higher ternary phosphide was obtained; the phosphorus excess always reacted with tin to generate Sn_4P_3 and SnP_3, which are soluble in HCl. A preliminary X-ray study (Weissenberg and precession photographs) showed the two types of crystals to have the same rhombohedral symmetry with Laüe group $\bar{3}$. No systematic absences were indicative of space group $R3$. The unit cell values within experimental errors did not vary from sample to sample. An X-ray pattern was obtained by crushing some crystals to a fine powder using a proportional counter diffractometer ($\lambda CuK\alpha$ radiation) (Fig. 2). The lattice constants are given in Table I. A microanalysis

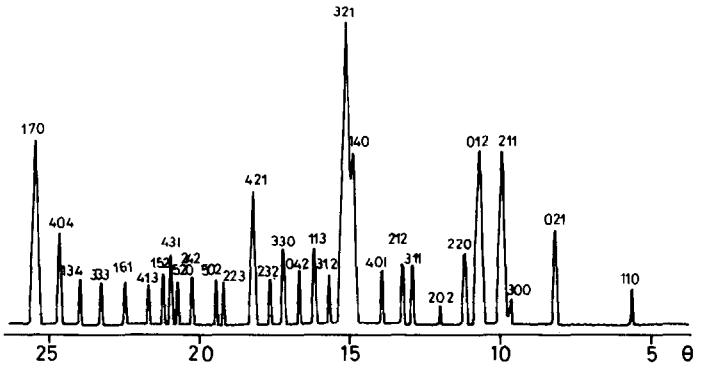

FIG. 2. X-ray pattern of $Sn_{4.2}Si_9P_{16}$ ($\lambda CuK\bar{\alpha}$) with hexagonal indices.

of different single crystals was carried out with a Camebax scanning electron microscope, employing energy of the X-ray spectrum emitted by the specimen. Two kinds of standards were used: either SiP and elementary tin or InP, Si^0, and Sn^0. the measurements were performed on 30 analysis points using a statistical precision given by Tixier formulation (*7*). The correction program was Corx (*8*) (Model ZAF (*9*)). Experimental and theoretical results are summarized in Table I.

TABLE I

EXPERIMENTAL AND THEORETICAL VALUES FOR $Sn_{4.2}Si_9P_{16}$

Physical, crystallographic, and analytical data
Formula: $Sn_{4.2}Si_9P_{16}$ Molecular weight: 1246.9
Theoretical weight fraction concentration (%): Sn, 41.5; Si, 21.3; P, 37.4
Microprobe analysis, average on 30 analysis points (%): Sn, 40.0; Si, 20.3; P, 39.8
Crystal symmetry: trigonal–rhombohedral
Space group: $R3$
Cell constants: a_R = 9.504(2) Å; α = 111.00(2)°; Z = 1
a_{Hex} = 15.665(3) Å; c_{Hex} = 8.761(4) Å; Z = 3
Density: d_{calc} = 4.30
Absorption factor: μ(λMo$K\alpha$), 77 cm^{-1}
Crystal size (mm^3): 0.08 × 0.06 × 0.06
Data collection and refinement conditions
Radiation: Mo$K\alpha$, 0.7107 Å
Scan method: $\omega - 2\theta$
Recording angle range: $1° < \theta < 28°$
Data collected: h, −12, +12; k, 0, +12; l, 0, +12
Number of unique reflections: 1010
Number of reflections $I > 3\sigma(I)$: 854
E.S.D. 1.04
Number of variables: 98
Extinction coefficient E_c: 9.98×10^{-8}
Structure solution: direct methods and Fourier
Refinement: full matrix least squares
Function minimized: $\Sigma_\omega(\|F_o\| - \|F_c\|)^2$
ω: $\frac{1}{4}\|(\sigma(I)^2/I + p^2I\|$ with p = 0.05
R: 0.027
R_ω: 0.034

Crystal Structure Determination

Single-crystal X-Ray data were recorded with an automated four-circle Enraf–Nonius CAD-4 diffractometer with graphite monochromated Mo$K\alpha$ radiation (Table I). Lorentz and polarization effects were taken into account as usual. After averaging equivalent reflections and omitting those for which $I < 3\sigma(I)$, 854 independent reflections were kept in refinement. The structure was solved by direct methods involving calculations of the normalized structure factors E and refined using the SDP package implemented on a PDP 11-60 minicomputer (*10*).

The first steps of refinement enabled us to locate 4 tin atoms in the 1a and 3d positions and 24 atoms first "called" phosphorus in eight sets of 3b positions, since phosphorus and silicon have quite equivalent electron weight. By considering the classical valence rules and distance calculations, these two elements were easily distinguished in the refinement. Several cycles of least-squares refinement which included isotropic temperature factors gave an R value of 0.078 (R_ω = 0.092). By introducing the anisotropic temperature factors, this value fell down to 0.058 (R_ω = 0.074). However a subsequent Fourier map revealed two additional peaks located on the 1a and 3b positions. The 1a position was attributed unambiguously to a tin atom with a partial occupancy factor (τ = 0.20 (*2*)). It appeared more difficult to choose between tin and phosphorus for the 3b position. However, excluding the ability of Sn–Sn bond distance shorter than 3 Å, which is twice the metallic radius of tin, this position was finally attributed to a phosphorus atom. In fact this position was partially occupied (τ = 0.33 (*2*)) and the final cycles including the occupancy factors together with the secondary extinction coefficient converged to the residual value of R = 0.027 (R_ω = 0.034), with quite correct thermal coordinates. The formula obtained was then $Sn_{4.2}Si_9P_{16}$. A final Fourier difference map

TABLE II

POSITIONAL AND THERMAL COORDINATES ($\beta \times 10^4$) OF $Sn_{4.2}Si_9P_{16}$

Atom	Position	x	y	z	β_{11}	β_{22}	β_{33}	β_{12}	β_{13}	β_{23}	B_{eq} (Å^2)
Sn(1)	1a	0	0	0	200.8(5)	200.8(5)	200.8(5)	360(1)	360(1)	360(1)	2.59(1)
Sn(2)	3b	0.47996(7)	0.31561(7)	0.73363(7)	49.8(6)	57.2(6)	76.0(6)	60(1)	74(1)	54(1)	1.39(1)
Sn(3)[a]	1a	0.5764(8)	0.5764(8)	0.5764(8)	82(4)	82(4)	82(4)	−2(1)	−2(1)	−2(1)	2.98(6)
Si(1)	3b	0.9275(3)	0.2489(3)	0.4647(3)	30(2)	33(2)	26(2)	35(4)	32(4)	34(3)	0.64(5)
Si(2)	3b	0.7878(3)	0.1466(3)	0.7281(3)	25(2)	35(2)	29(2)	37(3)	28(3)	40(3)	0.61(5)
Si(3)	3b	0.6288(3)	0.0419(3)	0.0002(3)	34(2)	30(2)	32(2)	39(3)	45(4)	33(4)	0.65(5)
P(1)	3b	0.7011(2)	0.2009(2)	0.5079(2)	29(2)	30(2)	22(2)	29(3)	28(3)	25(3)	0.62(4)
P(2)	3b	0.8862(3)	0.3022(2)	0.2474(2)	37(2)	35(2)	31(2)	37(3)	36(3)	46(3)	0.74(4)
P(3)	3b	0.0773(2)	0.7644(2)	0.5557(2)	41(2)	31(2)	29(2)	53(3)	41(3)	40(3)	0.64(4)
P(4)	3b	0.6592(3)	0.8100(3)	0.9094(3)	90(2)	68(2)	50(2)	126(4)	100(4)	95(3)	1.12(5)
P(5)	3b	0.3988(2)	0.9959(2)	0.0397(2)	34(2)	33(2)	25(2)	42(3)	38(3)	36(3)	0.62(4)
P(6)[a]	3b	0.352(1)	0.260(1)	0.188(1)	130(10)	110(10)	75(9)	120(20)	90(20)	100(10)	2.4(2)

Note. The form of the anisotropic parameter is: $\exp|-(\beta_{11}h^2 + \beta_{22}k^2 + \beta_{33}l^2 + \beta_{12}hk + \beta_{13}hl + \beta_{23}kl)|$. Estimated standard deviations are given in parentheses. $B_{eq} = \frac{4}{3}\Sigma_i\Sigma_j\beta_{ij}\mathbf{a}_i \cdot \mathbf{a}_j$.

[a] Occupancy factors: Sn(3): $\tau = 0.20(2)$; P(6): $\tau = 0.33(2)$.

TABLE III

MAIN INTERATOMIC DISTANCES (<3.40 Å) AND THEIR ESTIMATED STANDARD DEVIATIONS

Sn(1)–P(6)	2.669(11)	Si(1)–P(2)	2.233(3)
–3P(4)	2.681(3)	–P(1)	2.251(3)
		–P(5)	2.257(3)
Sn(2)–P(2)	2.650(3)	–P(1)	2.264(3)
–P(3)	2.663(3)		
–P(3)	2.688(2)	Si(2)–P(4)	2.223(4)
–P(6)	2.931(11)	–P(3)	2.254(3)
–3Sn(3)	3.350(7)	–P(5)	2.259(3)
		–P(1)	2.273(3)
Sn(3)–3P(4)	2.737(5)		
–P(6)	3.001(10)	Si(3)–P(4)	2.226(3)
–3Sn(2)	3.350(7)	–P(2)	2.236(4)
		–P(5)	2.266(3)
P(1)–Si(1)	2.251(3)	–P(3)	2.283(3)
–Si(1)	2.264(3)		
–Si(2)	2.273(3)	P(4)–Si(2)	2.223(4)
		–Si(3)	2.226(3)
P(2)–Si(1)	2.233(3)	–Sn(1)	2.681(3)
–Si(3)	2.236(4)	–Sn(3)	2.737(5)
–Sn(2)	2.650(3)		
–P(6)	2.686(10)	P(5)–Si(1)	2.257(3)
		–Si(2)	2.259(3)
P(3)–Si(2)	2.254(3)	–Si(3)	2.266(3)
–Si(3)	2.283(3)	–P(6)	2.685(11)
–Sn(2)	2.663(3)		
–Sn(2)	2.688(2)	P(6)–Sn(1)	2.669(11)
		–P(5)	2.685(11)
		–P(2)	2.686(10)
		–Sn(2)	2.931(11)
		–Sn(3)	3.001(10)

did not show any peak greater than 0.5 e/Å^3. The final positional and thermal coordinates are labeled in Table II; the main interatomic distances are given in Table III. The structure factor list will be sent on request.

Crystal Structure Description

Figure 3 illustrates the crystal structure of $Sn_{4.2}Si_9P_{16}$ which is of a new type. The structure is characterized by a 3D framework of $|SiP_4|$ tetrahedra with tunnels parallel to the |111| direction into which the tin atoms and one phosphorus atom, namely P(6), are inserted.

Weak P–P bonds occur in the structure in terms of one finite chain P(2)–P(6)–P(5) with P–P distances close to 2.68 Å. If such a distance compares favorably with those previously observed in the MnP-type phosphides (*13*), it appears about 20% larger than those usually reported for two-electron P–P bonds (2.22–2.24 Å) as in elementary phosphorus (*11, 12*) and polyphosphides (*14–16*).

The tin atoms have a typical coordination for Sn^{2+} with a stereoactive lone pair (Fig. 4). Indeed, the average bond lengths Sn–P of about 2.75 Å and the trigonal pyramidal

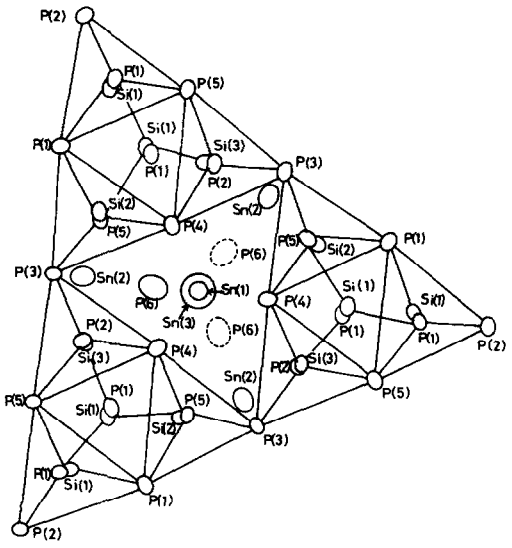

FIG. 3. Projection of the structure on the (001) plane of the hexagonal unit cell. Note that only one phosphorus P(6) really exists in the structure so that the phosphorus environment of tin atoms remains tetrahedral. The $|SiP_4|$ tetrahedra are emphasized.

$|SnP_3|$ configuration with bond angles covering the range from 77.3 to 85.8° together with the extension to a (3 + 1) coordination by a phosphorus atom at greater distance conform with the well-known coordination behavior of Sn(II) atoms and all electronically equivalent systems with a lone-pair configuration (*17, 18*). The Sn–P distances are comparable to those observed in SnP_3 (*19*), Sn_4P_3 (*20*), Cu_4SnP_{10} (*17*), and $CdSnP_{14}$ (*18*).

The silicon atoms have four close phosphorus neighbors which form a quite regular tetrahedron. The $|SiP_4|$ tetrahedra are running through the structure in a 3D arrangement by sharing apices. The Si–P bond distances cover the range from 2.223 to 2.283 Å with an average value of 2.252 Å which corresponds to the usual average bond lengths of 2.262 Å for Si–P bonds in $ZnSiP_2$ (*21*), K_2SiP_2 (*22*), Ba_4SiP_4 (*23*), and $AlSiP_3$ (*24*). The P–Si–P bond angles extend from 99.4 to 121.0° with an average value of 109.3° close to the ideal tetrahedral angle of 109.5° (Table IV). Thus the oxidation number of silicon atoms remains +4.

Physical Properties and Discussion

Single crystals of the two morphology types (needles or truncated octahedra) have been studied by electrical measurements. The experiments were performed by the

TABLE IV

MAIN ANGLE BONDS IN $|SiP_4|$ AND $|SnP_4|$ TETRAHEDRA ($\sigma \leqq 0.2°$)

P(1)–Si(1)–P(1) = 115.2	P(1)–Si(2)–P(3) = 102.9	P(2)–Si(3)–P(3) = 107.7
P(1)–Si(1)–P(2) = 111.6	P(1)–Si(2)–P(5) = 112.4	P(2)–Si(3)–P(4) = 113.4
P(1)–Si(1)–P(5) = 121.0	P(3)–Si(2)–P(5) = 107.0	P(2)–Si(3)–P(5) = 109.3
P(1)–Si(1)–P(5) = 101.8	P(1)–Si(2)–P(4) = 116.5	P(3)–Si(3)–P(4) = 104.1
P(1)–Si(1)–P(2) = 99.4	P(3)–Si(2)–P(4) = 105.4	P(3)–Si(3)–P(5) = 105.5
P(2)–Si(1)–P(5) = 105.1	P(4)–Si(2)–P(5) = 111.5	P(4)–Si(3)–P(5) = 116.1

P(4)–Sn(1)–P(4)	79.2 × 3	P(2)–Sn(2)–P(3)	83.1
P(4)–Sn(1)–P(6)	113.7	P(2)–Sn(2)–P(3)	85.8
P(4)–Sn(1)–P(6)	115.7	P(3)–Sn(2)–P(3)	85.0
P(4)–Sn(1)–P(6)	161.4	P(3)–Sn(2)–P(6)	154.3
		P(3)–Sn(2)–P(6)	111.4
P(4)–Sn(3)–P(4)	77.3 × 3	P(2)–Sn(2)–P(6)	116.7
P(4)–Sn(3)–P(6)	116.2		
P(4)–Sn(3)–P(6)	117.3		
P(4)–Sn(3)–P(6)	159.5		

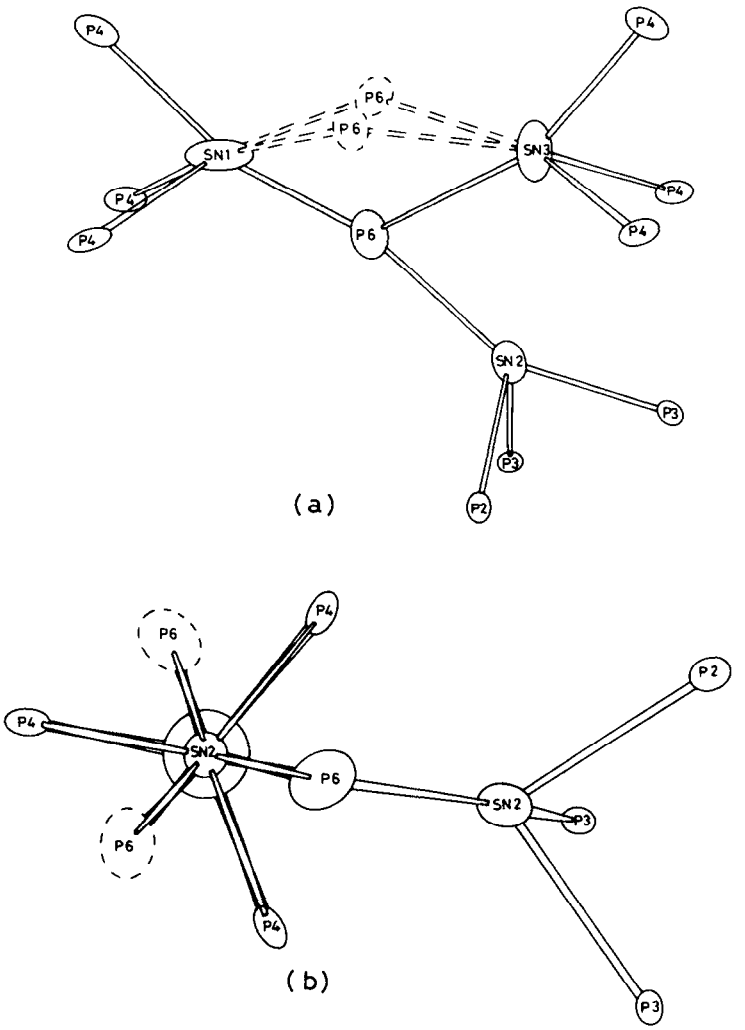

FIG. 4. The phosphorus environment of tin atoms viewed along (a) or perpendicular (b) to the |111| rhombohedral direction.

four-point method using silver-painted contacts and a direct current in the temperature range 150–293 K. As seen from Fig. 5, the curves $R/R_0 = f(T)$ are quite similar for both crystals and characteristics of a semiconducting behavior. The resistivity values have been determined on a needle about 0.40 mm long with a cross section $0.5 \times 10^{-2} \times 0.5 \times 10^{-2}$ mm^2; $Sn_{4.2}Si_9P_{16}$ has a low resistivity at room temperature, and the conductivity σ varies from 0.45 Ω^{-1} cm^{-1} at 293 K to 7×10^{-4} Ω^{-1} cm^{-1} at 150 K, i.e., by nearly three orders of magnitude. The slope of the curves $\ln (R/R_0) = f(10^3/T)$ corresponds to an activation energy $\Delta E \simeq 0.2$ eV which probably does not define the intrinsic behavior of the compound. The semiquantitative measurements of the thermoelectric effect at room temperature proves the conductivity to be electronic (n-type).

When applying the general valence rule for semiconductors $(n_c + e_a - e_c)/n_a = 8$ to $Sn_{4.2}Si_9P_{16}$ compound, the e_a value (number

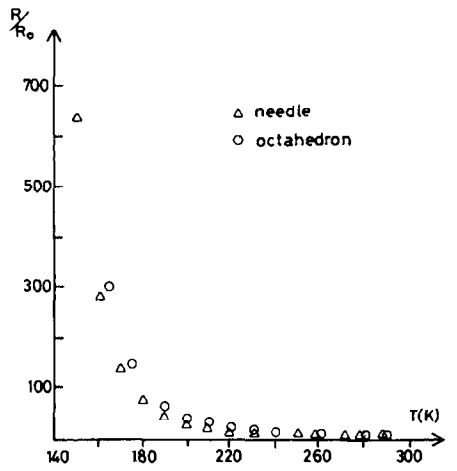

FIG. 5. Resistivity of $Sn_{4.2}Si_9P_{16}$ versus temperature.

of electrons involved in forming anion–anion bonds) is determined to be 3.6 electrons. (n_e, total number of valence electrons = 132.8; e_c, number of electrons involved in forming cation–cation bonds or any lone pairs = 8.4; n_a, number of anions = 16). Since two P–P bonds occur in the structure as a finite chain P_2–P_6–P_5, each P–P bond consequently needs 1.8 e^-. This result is in good agreement with the structure determination since P–P bond distances are larger than that expected for a 2-electron P–P bond.

Acknowledgments

The authors thank Dr. J. M. Claude and Dr. P. Steinmetz (Laboratoire de Chimie Minérale, Nancy) for the microprobe analysis.

References

1. F. HULLIGER AND E. MOOSER, *J. Phys. Chem. Solids* **24,** 283 (1963).
2. T. WADSTEN, *Acta Chem. Scand.* **21,** 593 (1967).
3. P. C. DONOHUE, W. J. SIEMONS, AND J. L. GILLSON, *J. Phys. Chem. Solids* **29,** 807 (1968).
4. T. K. CHATTOPADHYAY AND H. G. VON SCHNERING, *Z. Kristallogr.* **167,** 1 (1984).
5. T. WADSTEN, *Acta Chem. Scand.* **23,** 2532 (1969).
6. J. OSUGI, R. NAMIKAWA, AND Y. TANAKA, *Rev. Phys. Chem. Japan* **36,** 35 (1966).
7. M. ANCEY, F. BASTENAIRE, AND R. TIXIER, *J. Phys. D.* **10,** 817 (1977).
8. J. HENOC AND M. TONG, *J. Microsc. Spectrosc. Electron* **3,** 247 (1978).
9. R. BEAMAN AND J. A. ISASI, *Anal. Chem.* **42,** 1540 (1970).
10. B. A. FRENZ, The Enraf–Nonius CAD-4 SDP: A real time for concurrent X-ray data collection and crystal structure solution, *in* "Computing in Crystallography" (H. Schenk, R. Olthof-Hazekamp, M. Van Koningsveld and G. C. Bassi, Eds.), Univ. Press, Delft (1978).
11. A. THURN AND H. KREBS, *Acta Crystallogr. Sect. B* **25,** 125 (1969).
12. A. BROWN AND S. RUNDQVIST, *Acta Crystallogr.* **19,** 684 (1965).
13. R. GUÉRIN, M. SERGENT, AND J. PRIGENT, *Mater. Res. Bull.* **10,** 957 (1975).
14. U. FLÖRKE AND W. JEITSCHKO, *Inorg. Chem.* **22,** 1736 (1983).
15. R. GUÉRIN, M. POTEL, AND M. SERGENT, *Mater. Res. Bull.* **14,** 1335 (1979).
16. H. G. VON SCHNERING, W. WICKELHAUS, AND M. SCHULZE NAHRUP, *Z. Anorg. Allg. Chem.* **412,** 193 (1975).
17. W. HÖNLE AND H. G. VON SCHNERING, *Z. Kristallogr.* **153,** 339 (1980).
18. U. D. SCHOLZ AND W. JEITSCHKO, *J. Solid State Chem.* **67,** 271 (1987).
19. J. GULLMAN AND O. OLOFSSON, *J. Solid State Chem.* **5,** 441 (1972).
20. L. HÄGGSTRÖM, J. GULLMAN, T. ERICSSON, AND R. WÄPPLING, *J. Solid State Chem.* **13,** 204 (1975).
21. S. C. ABRAHAMS AND J. L. BERNSTEIN, *J. Chem. Phys.* **52,** 5607 (1970).
22. B. EISENMANN AND M. SOMER, *Z. Naturforsch. B* **39,** 736 (1984).
23. B. EISENMANN, H. JORDAN, AND H. SCHÄFER, *Mater. Res. Bull.* **17,** 95 (1982).
24. H. G. VON SCHNERING AND G. MENGE, *J. Solid State Chem.* **28,** 13 (1979).
25. W. B. PEARSON, *Acta Crystallogr.* **17,** 1 (1964).